Affinity grid-based cryo-EM of PKC binding to RACK1 on the ribosome

Gyanesh Sharma[1 ¶], Jesper Pallesen[1, 2 ¶], Sanchaita Das[1 ¶], Robert Grassucci[2], Robert Langlois[1,2], Cheri Hampton[1, 2], Deborah F. Kelly[4], Amedee des Georges[1, 2],and Joachim Frank[1, 2, 3, *]

[1]*Department of Biochemistry and Molecular Biophysics, Columbia University, New York, NY-10032, USA*

[2]*Howard Hughes Medical Institute, Department of Biochemistry and Molecular Biophysics, Columbia University, New York City, NY-10032, USA*

[3]*Department of Biological Sciences, Columbia University, New York City, NY-10032, USA*

[4]*Virginia Tech Carilion Research Institute, Roanoke, VA-24016, USA*

[¶]*Equal contributing Authors*

SUPPORTING INFORMATION

EXPERIMENTAL PROCEDURES

Preparation of 40S subunit bound to PKC βII

40S ribosomal subunits were purified according to Pisarev et *al*. (Pisarev et al., 2007). PKC βII (human) and its lipid activator were purchased from Millipore (catalogue number 14-496 and 20-133 respectively; Millipore, MA, USA). PKC βII contained an N-terminal His-tag. PKC βII was incubated with its lipid activator (1X) for 3 minutes at 30 ºC to activate it. 40S ribosomal subunits (75 nM) were

mixed with activated PKC βII (125 ng) at room temperature for 15 minutes in buffer solution containing (20 mM Tris pH 7.5, 2 mM DTT, 2 mM MgCl, and 100 mM KCl).

Preparation of Affinity Grid specimens

Lipid monolayers were prepared by adding ~30μL aliquots of Milli-Q water into the wells of Teflon blocks and overlaying each drop with a lipid mixture containing 1,2-dilauroyl-phosphocholine (DLPC) (Avanti Polar Lipids, AL, USA) and 1,2-dioleoyl-iminodiacetic acid-succinyl-nickel salt (Ni-NTA lipid) (Avanti Polar Lipids, AL, USA) (Kelly et al., 2008). Lipid mixtures were composed of 20% Ni-NTA lipids and 80% DLPC, each reconstituted to 1 mg/mL in chloroform. Teflon blocks were sealed in a humid petri dish and incubated on ice for 60 minutes prior to use. Quantifoil grids (Quantifoil Micro Tools, GmbH, Germany) composed of copper (200 mesh) and containing 2-μm holes separated by 2-μm of carbon spacing between holes were placed on top of each lipid monolayer sample and incubated for 1 minute. Each grid was then gently lifted off of each sample and the excess solution was removed using a Hamilton syringe. Sample aliquots (4 μL each) of the mixture containing 40S ribosomal subunits and activated PKC βII were incubated on each grid for 5 minutes at room temperature. Similarly, 4 μL samples containing just the apo-40S ribosomal subunit were incubated on an identical affinity grid for 5 minutes at room temperature. Specimens were loaded into an FEI Mark IV Vitrobot (FEI Company, OR, USA) and blotted for 3 seconds prior to plunging into liquid

ethane.

Electron Microscopy

The data were collected on a FEI Tecnai Polara electron microscope equipped with a field emission gun at a magnification of 59,000X under low dose conditions (~20 $e^-/Å^2$) using Kodak SO-163 film. 168 micrographs were collected manually and digitized using a Zeiss/Imaging scanner (Z/I Imaging Corporation, GmBH, Germany). The micrograph scans were decimated by a factor of 2 corresponding to a final pixel size of 2.82 Å on the object scale. Defocus for each micrograph was manually estimated using CTFMATCH (Huang et al., 2003). 30,397 particles were picked manually from 167 good micrographs using Orbweaver (Langlois et al., 2011). CTF-correction was performed at the level of raw data. The data set was processed with SPIDER through a protocol selecting only a subset of well-aligned particles (as determined by cross-correlation coefficient) in every view for reconstruction in each round of refinement. Throughout refinement, we employed SIRT reconstruction (conjugate gradients method) combined with regularization. The resolution of the final map obtained by using the total dataset was estimated at 11.4 Å with the Fourier Shell Correlation 0.5 criterion (Figure S1). Following convergence of refinement, we used focused alignment (Brignole and Asturias, 2010; Burgess et al., 2004) to bring PKC βII exhibiting varying orientations into register. To this end, we applied a globular mask with a Gaussian fall-off to our density map such that it encompassed RACK1 and part of the 40S head density, as well as the surroundings of RACK1. We then allowed the particle coordinates

to “breathe” by allowing +/- 1 pixel of translational and +/- 2 degrees (1 degree sampling grid) of rotational change for two rounds of refinement to the masked density map. This procedure was followed by two rounds of refinement (parameters as described above) to the density map (this time without mask). As a negative control, we placed an identical mask elsewhere and performed alignment/refinement as described above.

Docking of RACK1 to PKC-40S cryo-EM map

Rigid body docking of RACK1 from *H. sapiens* in the PKC-40S density map was performed in UCSF Chimera using as guide the atomic model of the ribosome from *Canis lupus familiaris* (PDB ID 2ZKQ) (Pettersen et al., 2004).

SUPPLEMENTAL INFORMATION

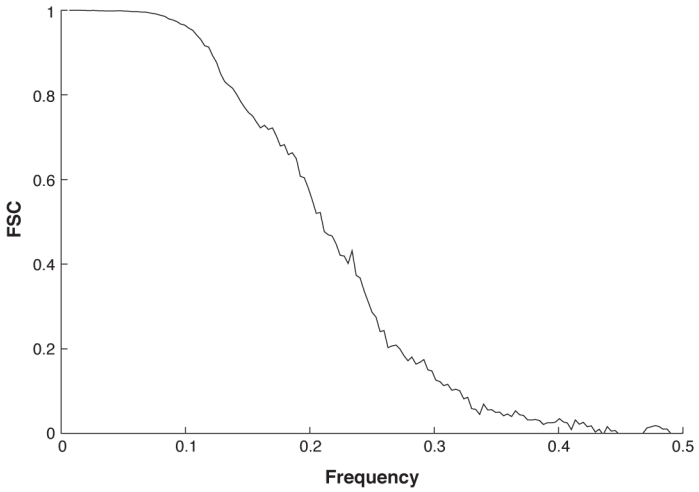

Figure S1. Fourier Shell Correlation for the PKC-40S complex after Refinement.

The graph represents the Fourier shell correlation (FSC) indicating a resolution of 11.4 Å, using the 0.5 FSC criterion.

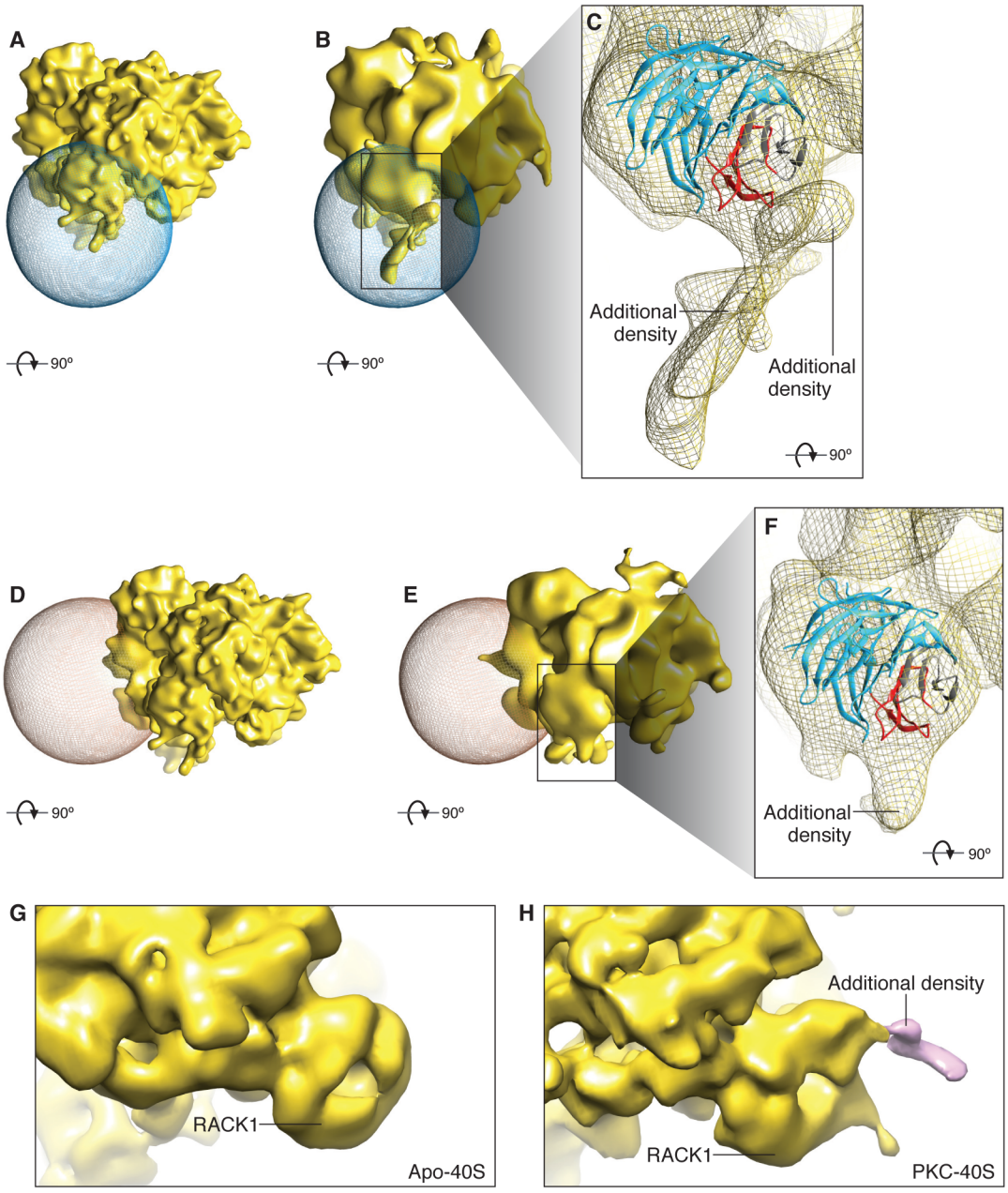

Figure S2. Density map of PKC-40S and Focused Alignment, rotated 90°

(A) Complex presented in Figure 2D, rotated by 90° around the abscissa; (B) corresponds to Figure 2E and (C) to Figure 2F. For the control experiment, (D) corresponds to Figure 2G rotated by 90 degrees around the abscissa; (E) to Figure 2H and (F) to Figure 2I. (G) Apo-40S ribosomal subunit segmented from

an 80S cryo-EM map filtered to 11.4Å (Budkevich et al., 2011). (H) Complex in Figure 2A, rotated by 90° around the abscissa, showing the presence of additional density bound to RACK1. (The other protrusion from RACK1 is due to the C-terminal tail of ribosomal protein rpS3e, according to (Rabl et al., 2011).

Figure S3. Orientation averages of projection images.

Projection images were averaged after being sorted into 100 view-directions based on orientation parameters obtained in refinement (in accordance with the analysis presented in Figure 3). The six overrepresented views are highlighted and labeled in orange. Note that the montage contains only averages

corresponding to reference projections on the upper orientation half-sphere; reference projections on the opposite hemisphere are related by mirroring around a vertical axis in the plane of the averages. For an in-depth treatment of orientation parameters for the full Euler-sphere, consult Figure 3.

REFERENCES

Brignole, E.J., Asturias, F., 2010. Single-particle electron microscopy of animal fatty acid synthase describing macromolecular rearrangements that enable catalysis. Methods Enzymol 483, 179-202.

Budkevich, T., Giesebrecht, J., Altman, R.B., Munro, J.B., Mielke, T., Nierhaus, K.H., Blanchard, S.C., Spahn, C.M., 2011. Structure and dynamics of the mammalian ribosomal pretranslocation complex. Molecular cell 44, 214-224.

Burgess, S.A., Walker, M.L., Thirumurugan, K., Trinick, J., Knight, P.J., 2004. Use of negative stain and single-particle image processing to explore dynamic properties of flexible macromolecules. Journal of structural biology 147, 247-258.

Huang, Z., Baldwin, P.R., Mullapudi, S., Penczek, P.A., 2003. Automated determination of parameters describing power spectra of micrograph images in electron microscopy. Journal of structural biology 144, 79-94.

Kelly, D.F., Dukovski, D., Walz, T., 2008. Monolayer purification: a rapid method for isolating protein complexes for single-particle electron microscopy. Proc Natl Acad Sci U S A 105, 4703-4708.

Langlois, R., Pallesen, J.,Frank, J., 2011. Reference-free particle selection enhanced with semi-supervised machine learning for cryo-electron microscopy. Journal of structural biology 175, 353-361.

Pettersen, E.F., Goddard, T.D., Huang, C.C., Couch, G.S., Greenblatt, D.M., Meng, E.C., Ferrin, T.E., 2004. UCSF Chimera--a visualization system for exploratory research and analysis. J Comput Chem 25, 1605-1612.

Pisarev, A.V., Unbehaun, A., Hellen, C.U., Pestova, T.V., 2007. Assembly and analysis of eukaryotic translation initiation complexes. Methods Enzymol 430, 147-177.

Rabl, J., Leibundgut, M., Ataide, S.F., Haag, A., Ban, N., 2011. Crystal structure of the eukaryotic 40S ribosomal subunit in complex with initiation factor 1. Science 331, 730-736.